Biomed Microdevices (2010) 12:1–12
DOI 10.1007/s10544-009-9352-2

Microfluidic gradient PCR (MG-PCR): a new method for microfluidic DNA amplification

Chunsun Zhang · Da Xing

Published online: 15 September 2009

Abstract This study develops a new microfluidic DNA amplification strategy for executing parallel DNA amplification in the microfluidic gradient polymerase chain reaction (MG-PCR) device. The developed temperature gradient microfluidic system is generated by using an innovative fin design. The device mainly consists of modular thermally conductive copper flake which is attached onto a finned aluminum heat sink with a small fan. In our microfluidic temperature gradient prototype, a non-linear temperature gradient is produced along the gradient direction. On the copper flake of length 45 mm, width 40 mm and thickness 4 mm, the temperature gradient easily spans the range from 97 to 52°C. By making full use of the hot (90–97°C) and cold (60–70°C) regions on the temperature gradient device, the parallel, two-temperature MG-PCR amplification is feasible. As a demonstration, the MG-PCR from three parallel reactions of 112-bp *Escherichia coli* DNA fragment is performed in a continuous-flow format, in which the flow of the PCR reagent in the closed loop is induced by the buoyancy-driven nature convection. Although the prototype is not optimized, the MG-PCR amplification can be completed in less than 45 min. However, the MG-PCR thermocycler presented herein can be further scaled-down, and thus the amplification times and reagent consumption can be further reduced. In addition, the currently developed temperature gradient technology can be applied onto other continuous-flow MG-PCR systems or used for other analytical purposes such as parallel and combination measurements, and fluorescent melting curve analysis.

Keywords Microfluidic gradient PCR (MG-PCR) · Microfluidic DNA amplification · Continuous-flow · Temperature gradient · Nature convection

C. Zhang · D. Xing (✉)
MOE Key Laboratory of Laser Life Science & Institute of Laser Life Science, College of Biophotonics,
South China Normal University,
No.55, Zhongshan Avenue West, Tianhe District,
Guangzhou 510631, People's Republic of China
e-mail: xingda@scnu.edu.cn

1 Introduction

The polymerase chain reaction (PCR) technique represents a major advance in molecular biology. It has been applied to a diverse range of basic research and application fields, including medical diagnostics, infectious and hereditary disease detection, forensic science, and genomics. Under optimal conditions, the PCR is very efficient; microgram quantities can be synthesized from a single-molecule DNA template. Optimization of PCR involves testing a number of variables, one of which is the primer annealing temperature. Although good primers are chosen, i.e., those that do not form dimmers by annealing of their 3′-termini and that are specific to one sequence in template DNA, annealing temperature optimization is important for PCR performance (Rychlik et al. 1990; Wu et al. 1991). If the annealing temperature is too low, non-specific DNA fragments are amplified, causing the appearance of multiple bands on agarose gels. If it is too high, the yield of the desired product, and sometimes the product purity is decreased due to poor annealing of primers (Rychlik et al. 1990). Fortunately, commercial gradient PCR machines can generate a temperature gradient up to 12 different annealing temperatures, and they have been successfully used in many fields such as site-directed mutagenesis (Padmakumar and Varadarajan 2003), improvement of the efficiency and reliability of RT-PCR using tag-extended primers (Sybesma

et al. 2001), and identification of *Panax* Species in the herbal medicine preparations (Shim et al. 2005). However, conventional gradient PCR machines tend to be expensive; make a gradient up to only 12 different annealing temperatures spanning a range of 20°C. Recently, Chang and Lee have developed a volumed gradient PCR method, in which a traditional PCR machine can be converted into a gradient PCR machine (Chang and Lee 2005). Although this strategy can make as many annealing temperatures as possible by adjusting reaction volume, the accuracy of annealing temperature largely depends on one of titered volumes that may vary among users. In addition, the reaction volume also affects the specificity of DNA amplification, as similar to the annealing temperature does. Importantly, conventional PCR cycles are performed in a metal block thermal cycler that usually takes 2–3 h for thirty cycles; most of the reaction time is spent on cooling and heating during the reaction process. In addition, these PCR machines are bulky and energy intensive, making it hard to bring PCR (including gradient PCR) to point-of-care (POC) applications.

In recent years, great effort has been spent in miniaturizing the PCR technique in order to increase reaction throughputs and small-scale integration level while simultaneously minimizing reagent consumption and/or reaction time (Zhang et al. 2006, 2007a; Zhang and Xing 2007). The design and operation of microfluidic PCR can be classified into two principal categories: stationary chamber-based PCR and dynamic flow-based PCR. Originally, chamber-based PCR is performed in a PCR solution-containing chamber that is cycled between different temperatures (Wilding et al. 1994). Subsequently, the array chambers on a single chip have been developed for high-throughput DNA amplification and analysis (Fan and Quake 2007; Morrison et al. 2006; Nagai et al. 2001). This chamber-based stationary approach can produce PCR systems with the smallest footprint and the highest integration, but complex control instrumentation is required to thermally cycle the PCR solution among the desired temperatures. In addition, the thermal mass associated with the heater, PCR chamber and solution usually limits the flexibility to change the PCR speed.

Alternatively, the dynamic flow-based PCR performs DNA amplification by using the 'time-space conversion' concept. The amplification reaction occurs as the DNA sample continuously flows through a microfluidic channel during each temperature cycle. The entire PCR period depends only on the sample flow rate and the time needed for the sample to reach a thermal equilibrium. In 1998, Kopp et al. reported a continuous-flow PCR chip using a microfluidic serpentine channel embedded within a glass substrate (Kopp et al. 1998). Since then, some researchers have continued to improve the operation of this original device (Zhang et al. 2006, 2007a; Zhang and Xing 2007). Importantly, continuous-flow PCR for high-throughput applications has been developed in a serial (Chabert et al. 2006; Curcio and Roeraade 2003; Dorfman et al. 2005; Kiss et al. 2008; Li et al. 2009; Obeid et al. 2003; Park et al. 2003; Schaerli et al. 2009; Zhang et al. 2007b) or parallel (Sun et al. 2008) format. For serial high-throughput amplification, either the sample can be a droplet entrained in an immiscible solvent (Chabert et al. 2006; Curcio and Roeraade 2003; Dorfman et al. 2005; Kiss et al. 2008; Schaerli et al. 2009), or numerous aqueous sample plugs can be separated by plugs of air (Li et al. 2009; Obeid et al. 2003; Park et al. 2003; Zhang et al. 2007b). For example, Dorfman et al. examined continuous-flow PCR using droplets in an immiscible, fluorinated solvent flowing in Teflon capillaries, without any detectable contamination between neighboring droplets (Dorfman et al. 2005). Park et al. demonstrated a segmented-flow PCR of four different samples for amplifying different DNA fragments (500, 323, 497, and 267 bp), where the air gap/bromophenol blue buffer plug/air gap was interposed between each sample to discourage the carryover from one segment to the following one. In the parallel format, different samples are amplified in different continuous-flow reaction channels. For example, Sun et al. recently reported a multichannel closed-loop magnetically actuated microchip for high-throughput, continuous-flow PCR (Sun et al. 2008). Four different genes, the 172-bp 35 S-promoter sequence that is specific for the detection of genetic modifications in soybeans, the soybean control 118-bp lectin gene *LE*1 that is detectable in both transgenic and conventional soybeans, the 211-bp *cry*IA gene specific for the transgenic maize, and the 226-bp invertase maize control gene were amplified simultaneously in the four different channels of the microchip, and 25 cycles were completed within 13 min. However, all these high-throughput PCR amplification and analysis systems (including stationary array chamber-based PCR and dynamic flow-based PCR (serial and parallel)) performed PCR of different samples using the same annealing temperature. In general, performing PCR for various gene segment amplifications from different template samples and/or different primer pairs requires different annealing temperatures, and an optimized annealing temperature can give a more effective and specific DNA amplification. Therefore, in order to effectively perform high-throughput PCR amplifications by microfluidic PCR, the annealing temperatures among different PCR reactions should be closely controlled, just like the conventional gradient PCR machine does.

We present here a microfluidic gradient PCR (MG-PCR) method for performing parallel DNA amplifications with different annealing temperatures. This is accomplished by using an innovative temperature gradient microfluidic system. When high temperatures (for example 90–97°C)

and low temperatures (for 52–68°C) on the developed planar thermal gradient device are used for PCR temperatures, the two-temperature MG-PCR can be achieved. Here, as a demonstration and proof of principle, three-parallel PCR reactions with various annealing/extension temperatures were tested using the same gene segment to be amplified, where the flow of the PCR reagent in the closed-loop PCR reaction was driven by the buoyancy-driven nature convection. As the research background of our study and potential applications of our microfluidic temperature gradient technique, the other temperature gradient devices for microfluidic DNA analysis also have been introduced.

2 Temperature gradient devices for microfluidic DNA analysis

Over the last several years, the development of the temperature gradient microfluidic devices has attracted great interest, and has witnessed steady advances. Early in 2003, Kajiyama et al. demonstrated a temperature gradient DNA microarray hybridization chip for genotyping of four different loci in two genes (Kajiyama et al. 2003). Silicon-based chips with discrete, independently temperature-controlled islands were developed and temperatures at each island could be set at different values to obtain optimal distinction between perfect matches and mismatches (Kajiyama et al. 2003). Traditionally, DNA melting analysis is a time-based process. A recent technique, spatial DNA melting analysis, can detect fluorescence as a function of position instead of time, by creating a characteristic gradient within the DNA sample. Performing spatial DNA melting analysis in a temperature gradient device was first demonstrated by Mao et al. (Mao et al. 2002a, b). They utilized a poly(dimethylsiloxane) (PDMS) (Mao et al. 2002b) or glass (Mao et al. 2002a) substrate containing multiple microchannels that were each heated to a unique temperature on a linear temperature gradient device. In order to detect single nucleotide polymorphisms (SNPs), the channels were first filled with a concentrated solution containing a DNA dye and double-stranded oligonucleotides (30-bp) (Mao et al. 2002a). A similar method was also demonstrated by Baaske et al. (Baaske et al. 2007), where an infrared laser was used to generate a radial temperature gradient distribution between 20 and 100°C within a small (10 nl) volume. The thermal denaturing of a concentrated sample containing a dye-labeled DNA hairpin (33-bp) was performed in a snapshot (50 ms). Different from these two prior studies, Crews et al. recently reported simultaneous continuous-flow PCR amplification and spatial melting curve analysis starting from the non-designed and non-synthesized DNA templates within a one-dimensional linear temperature gradient (Crews et al. 2008a, c, 2009). The denaturing of the PCR product during each cycle was monitored by imaging the continuous-flow PCR on the temperature gradient device. A similar demonstration was also performed by Kinahan et al. (Kinahan et al. 2009), who measured DNA melting temperatures from two plasmid fragments within a linear temperature gradient to study the effects of substrate thermal resistance (including flow velocity and ramp-rate) on continuous-flow microchannel melting curve analysis. It should be noted that some temperature gradient microfluidic devices have been incorporated onto the chip-based capillary electrophoresis systems to perform DNA mutation detection (Zhang et al. 2007c; Buch et al. 2004, 2005), and microfluidic temperature gradient focusing (Balss et al. 2004; Ross and Locascio 2002).

Recently, the temperature gradient technique has been used for the continuous-flow PCR applications. By using this technique, the original chip-based continuous-flow PCR device reported by Kopp et al. has been improved to a certain extent. For example, Crews et al. used a microfluidic serpentine channel embedded within a glass substrate, as similar to Kopp et al.'s work, and substituted a single steady-state temperature zone for three distinct temperature zones reported by Kopp et al.. As a result, the serpentine channel continuous-flow PCR chips on a temperature gradient device were performed (Crews et al. 2007, 2008b). In their device, the spatial distribution of the required PCR temperatures can be significantly decreased, resulting in a much smaller chip footprint. In addition, by reducing two-dimensional isothermal areas into one-dimensional isothermal lines, residence time can be eliminated. Very recently, a similar study has been demonstrated by Schaerli et al. (Schaerli et al. 2009). They integrated the circular design of the serpentine channel onto a radial temperature gradient to perform the continuous-flow PCR of single-copy DNA in microfluidic microdroplets. Heating from the center established a natural temperature gradient across the device. The gradient can be externally adjusted via an annular Peltier module that can be heated or cooled according to requirements of the template and primers. Early in 2005, this radial temperature gradient has been used by Cheng et al. for performing the oscillatory-flow PCR where the reagents was pumped back and forth along the radial direction of the chip to achieve rapid temperature cycling, maintaining the flexibility of varying the cycle number and varying the number of temperature zones (Cheng et al. 2005). A similar oscillatory-flow PCR on a linear temperature gradient was recently reported by Ohashi et al. (Ohashi et al. 2007), who used the magnetic transportation to move the PCR reaction droplets to the designated temperature zones on a linear temperature gradient from 50°C to 94°C. Other dynamic flow-based PCR systems induced by a temperature gradient have been reported elsewhere (Braun et al. 2003; Duhr and

Braun 2006; Grover et al. 2008; Krishnan et al. 2002; Stoffel et al. 2007). However, all these flow-based PCR systems performed on a temperature gradient *do not* fall into the category of MG-PCR unless they meet the requirements of the MG-PCR concept described below.

3 Concept of microfluidic gradient PCR (MG-PCR)

The concept of MG-PCR can be described as follows. First, the PCR reactions should be performed in a microfluidic format, including dynamic flow-based PCR and stationary chamber-based PCR. The beautiful operation of regents at the microscale level possibly allows MG-PCR to but not limited to integrate with other upriver and/or downriver functional modules, and to amplify and analyse template samples in a shorter time. Second, the multiple PCR reactions can be perform in a parallel (or high-throughput) fashion. Presently, advances in the field of micro-electro-mechanical-systems (MEMS) allow the ultra-high throughput array chip to be fabricated in a PDMS (Fan and Quake 2007), silicon (Nagai et al. 2001), and even 317 stainless steel (Morrison et al. 2006) substrate. Compared with conventional 96-chamber gradient PCR, this microfluidic feature may be attractive. Third, each reactor or each reactor group has a distinct, independently-controlled annealing temperature by using the temperature gradient technique. When these three features are realized at the same time, a MG-PCR method will be established. Figure 1 shows the schematic diagram of the stationary chamber-based MG-PCR (Fig. 1(a)) and the dynamic flow-based MG-PCR (Fig. 1(b)) concept.

4 Experimental section

4.1 Reagents and materials

10 × Taq DNA polymerase buffer (500 mM KCl, 100 mM Tris-HCl (pH 8.8), 0.8% Nonider P-40), $MgCl_2$ solution (25 mM), and thermostable Taq polymerase (5 unit/μl) were purchased from Bio Basic Inc. (BBI) (Ontario, Canada). Deoxynucleotide triphosphate (dNTPs) (10 mM each of dATP, dGTP, dCTP, and dTTP in water), PCR primers, and agarose were obtained from Shanghai Sangon Biological Engineering & Technology Services Co. Ltd. (SSBE) (Shanghai, China). Forward and reverse primer sequences were 5′ -GGA ATC AGG CGT CTG GGT CA-3′ and 5′ -GCC GTT AGT CGC TTC GTC ATA-3′, respectively. The doubly deionized H_2O (ddH_2O) were purchased from Tiangen Biotech Co. Ltd. (Beijing, China).

Bovine serum albumin (BSA) (fraction V, purity ≥98%, biotechnology grade, Cat. No. 735094), which was used to dynamically passivate the inner surface to decrease the surface adsorption, was purchased from Roche Diagnostics GmbH (Mannheim, Germany). Sodium hypochlorite solution, which was utilized to remove the residual substance from the microchannel before each run, was obtained from Guanghua Chemical Factory (Guangzhou, China). The DNA markers, which contain 2000, 1000, 750, 500, 250, and 100-bp DNA fragments, were bought from Win Honor Bioscience (Beijing, China). GoldView™ dye was purchased from SBS Genetech Co. Ltd. (Beijing, China). The polytetrafluoroethylene (PTFE) capillary tube (inner diameter 500 μm) was purchased from Wuxi Xiangjian Tetrafluoroethylene Product Co. Ltd. (Wuxi, China). The silicone tube was from Jinan Chen Sheng Medical Silicone Rubber Products Co., Ltd. (Jinan, China).

4.2 Design of temperature gradient platform

In our work, an innovative combined fin design is utilized to produce a desired temperature gradient for MG-PCR. Figure 2(a) is the illustration of the concept of a non-linear temperature gradient microfluidic system. Here, T_b at the x=0 is the temperature of the fin base, L, H, and δ denote the length, height, thickness of the fin, respectively. h is the overall heat-transfer coefficient based on the fin surface and T_∞ is the ambient temperature. In the single fin system, the

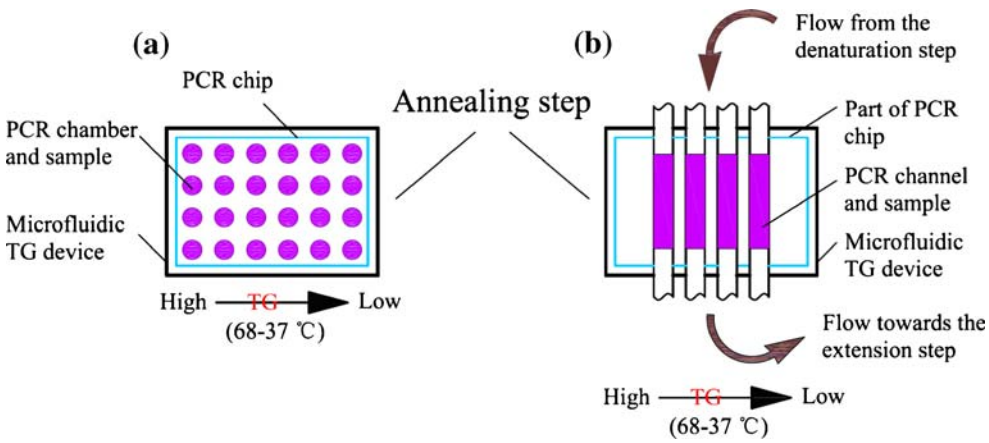

Fig. 1 Schematic diagram of the MG-PCR concept. **(a)** Stationary chamber-based MG-PCR. **(b)** Dynamic flow-based MG-PCR. TG = temperature gradient

equation governing heat transfer can be expressed as $\theta(x) = C_1 e^{ax} + C_2 e^{-ax}$, where $\theta = T - T_\infty$ is the temperature excess, α equals $(hp/kA)^{1/2}$ (here, p is the perimeter length of the fin $(p = 2*(H+\delta))$, k is the thermal conductivity of the fin material, A is the cross-sectional area of the fin at location x), C_1 and C_2 are arbitrary constants whose values are contingent upon the boundary conditions at the base and at the tip of the fin. From the governing equation, the temperature along the fin decreases exponentially from T_b to a certain value, as illustrated in Fig. 2(b). This equation also states that larger α results in smaller θ under the same conditions. That is, heat transfer in the fin is enhanced, and temperature gradient is easily produced. For a given fin material, the α mainly depends on the h and A. In our fin array, the A keeps constant, and the desired temperature gradient can be obtained by changing the h value and by use of the combined fin array design. Within the combined fin, some fins are evenly attached to another fin where the temperature gradient for MG-PCR exists.

4.3 Temperature gradient device assembly and operation

To evaluate the MG-PCR, a compact temperature gradient device was constructed by simply assembling together the glass cover, grooved copper flake, fin array heat sink, copper heat block hollowed out with a circular hole (8 mm diameter), resistance cartridge heater (100 W, 8 mm×40 mm (o.d. × length), Guangzhou Haoyi Thermal Electronics Factory, Guangzhou, China) and fan (Model DFB0412L, Delta Electronics Inc., Taiwan, China). Figure 3 is the photograph of the assembled temperature gradient device. The heat sink, grooved flake, glass cover, and heating block were fabricated by Automation Engineering R&M Centre (AERMC), Guangdong Academy of Sciences (Guangzhou, China). The copper flake is 72 mm long, 40 mm wide, and 4 mm deep, where the eighteen parallel grooves of 1.1 mm width and 1.1 mm depth are formed and covered an area of 40 mm×45 mm. The fin array heat sink has seven aluminum fins (each 16 mm high and 1.6 mm thick), which were evenly laid on the 2.5-mm-thick aluminum flake in a parallel fashion. The grooves on the copper flake were covered with a glass cover whose edges are in contact with a raised piece of the copper flake. Such design can improve temperature uniformity within the loop reactor. The heating block, heat sink, and glass cover were adhered to the temperature gradient flake by screws with low thermal conductivities. It should be noted that a small amount of thermally-conductive adhesives (Model HZ-DR3219, Wuxi Lily Adhesion Agent Factory, Wuxi, China) were applied between these contacting thermal elements to ensure uniform thermal contact and a good temperature gradient distribution. The fan was bound to the fined heat sink by four threaded screws and was powered by a DC supply (Model PS-305D, Longwei Instrument Meter Co. Ltd., Hongkong, China).

The desired steady-state temperature gradient in the device is obtained by running the heater and the fan. The heater supplies the amount of heat applied to the hotter edge of the temperature gradient flake, and the heat sink blown by the fan withdraws the heat from the copper flake. As a result, the temperature gradient can be well adjusted. A thermocouple (K-type, 0.005 inch diameter, Omega Engineering Inc., Stamford, CT, USA) was inserted into the bore of the copper flake near the first groove to probe its temperature. Similar thermocouples were also used to measure the temperatures within grooves. Through a terminal block (TBX-68 T, National Instruments Corp., Austin, TX, USA), the thermocouple was connected to a data acquisition system (PCI 4351, National Instruments Corp., Austin, TX, USA) that converted the analog signal to the digital one. A computer received the temperature signal through a PCI-4351 interface and determined the power input to the heater using a fuzzy proportional/integral/derivative (PID) algorithm that was programmed with LabView (Version 8.0, National Instrument Corp., Austin, TX, USA). Figure 4 is a schematic diagram of the microfluidic gradient PCR thermocycler set-up.

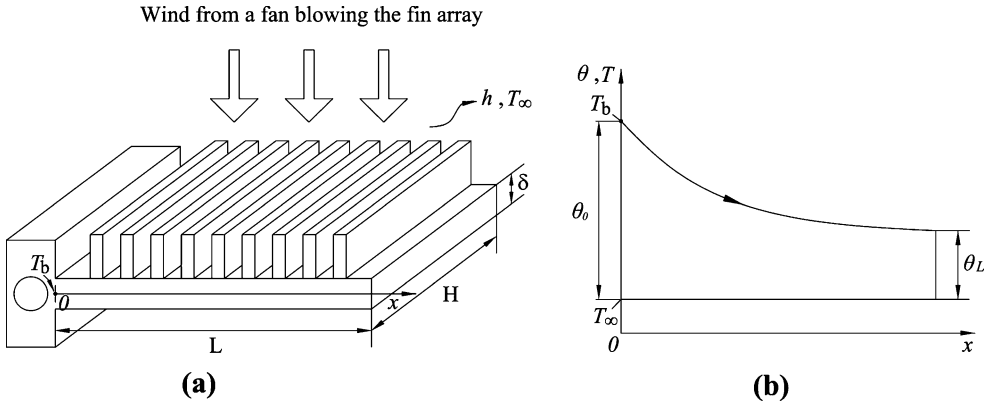

Fig. 2 Illustration of the concept of a non-linear temperature gradient microfluidic system. **(a)** Combined fin design to which a cooling fan is attached. **(b)** The temperature varies exponentially along the fin flake

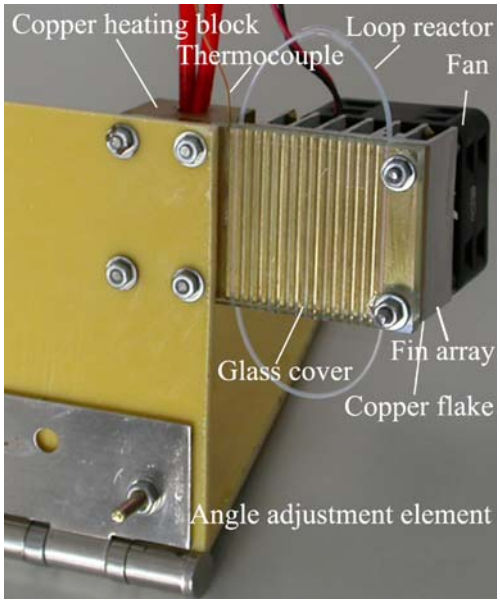

Fig. 3 Photograph of the assembled temperature gradient device

The convective loop reactor was constructed by using the PTFE tubing. After a PTFE tube was fitted into the grooves at the hot and cold part of the temperature gradient device, it was bent to nearly the shape of a "0" (Fig. 3). The length of each vertical side is 40 mm. The total length and volume of the loop are 180 mm and 35 μl, respectively. It is demonstrated later that these dimensions can be further reduced. Lengths of tubing were filled with PCR solutions and then the ends of the tubing were joined by using a sleeve of silicone tube. Slightly overfilling the fluid loop prior to jointing the two open ends can prevent bubble formation. In our prototype, the upper and lower parts of the tube were insulated in order to ensure the two-temperature convective PCR. During each experiment, the arrangement of the heater or the form of temperature gradient facilitated clockwise circulation in the fluid loop, and an ambient temperature of 22°C was maintained, and its variation was within ± 0.5°C. Additionally, the device was inclined to an angle (α) of 60° with respect to the horizontal. Of course, this angle can be varied according to the actual PCR experiments. For example, when a longer DNA template is amplified, the α should be smaller. On the contrary, the amplified DNA segment is shorter, the α should be larger. In addition, when the diameter of the loop is smaller, the α can be adjusted to 90° for use.

After introduction of the solution, the temperature at the bore location was heated to 97°C and maintained 5 min to ensure initial denaturation. Subsequently, a 4–12 V voltage was applied to the fan to execute the convective PCR. After some cycles, the temperature was decreased to 76°C, and then the fan stopped working. This temperature maintained for 6 min to complete final extension.

4.4 PCR experiments

To demonstrate the capability of the MG-PCR, small targets were amplified from *E. coli* K12 genomic DNA, and the amplified product is a 112-bp fragment out of 1194-bp tyrB gene. Both the control PCR and MG-PCR solutions used for amplification consisted of 0.5 μM of each primer, 0.2 mM of each dNTP, 0.1 unit/μl Taq DNA polymerase, 4 ng/μl DNA templat, 1.5 mM $MgCl_2$, 1 × Taq DNA polymerase buffer and 250 ng/μl BSA. To compare amplification characteristics (speed, specificity, and yield), portions of each PCR solution were amplified in both the MG-PCR device and commercial Mastercycler gradient PCR thermocycler (Eppendorf AG, Hamburg, Germany). To validate the amplification, negative controls (without template DNA or Taq enzyme) were amplified to ascertain if the amplification results from residual contamination. For MG-PCR reactions, the amplification times were 120, 90, 60, 45, and 30 min (not including the initial denaturation and final extension times). In the bench-top PCR thermocycler, two kinds of PCR protocols were used: three-temperature PCR and two-temperature PCR. The former consisted of 3-min denaturation at 94°C, 35 cycles (0.5 min at 94°C, 0.5 min at 60°C, and 1.5 min at 72°C), and final extension at 72°C for 3 min, which gave a total run time of 100 min including temperature ramping times. Two-temperature PCR was programmed for an initial denaturation step of 3 min at 94°C, followed by 35 cycles of 0.5 min at 94°C, 1 min at 60–70°C, and a final extension at 60–70°C for 3 min, with a total run time of 50 min including temperature ramp times. PCR results of positive and negative controls were analyzed on a 1.2 % agarose gel

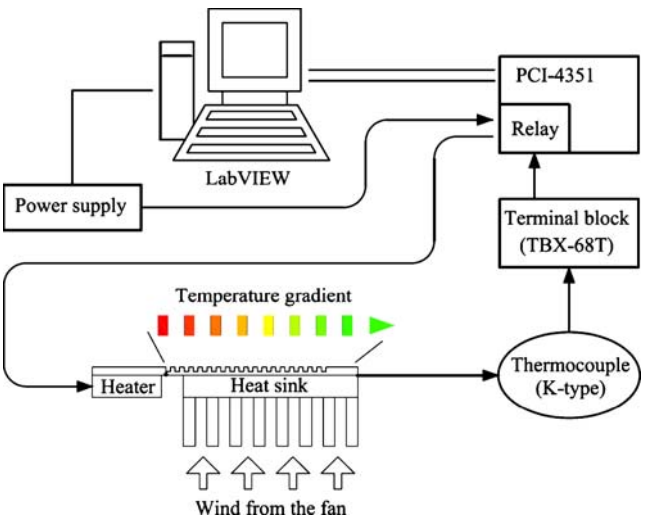

Fig. 4 A schematic diagram of the microfluidic gradient PCR thermocycler set-up. The convective-flow PCR loop reactor is embedded within the grooves on the temperature gradient copper flake controlled with a LabVIEW program

containing GoldView™ dye. Gels were typically run at 125 V for 35 min.

5 Results and discussion

5.1 Evaluation of temperature gradient

In most of the above-mentioned temperature gradient devices for microfluidic DNA analysis applications, the principle of their working exploits the fact that heat flow in two dimensions between a heat source and cold sink leads to a linear temperature gradient between the two when they are placed in parallel (Cheng et al. 2005; Crews et al. 2007, 2008a, b, c, 2009; Kinahan et al. 2009; Mao et al. 2002a, b; Ohashi et al. 2007; Ross and Locascio 2002; Schaerli et al. 2009). For example, within Ross and Locascio's work, the temperature gradient was produced by thermally anchoring the thin polycarbonate microchannel chips to alternatively heated or cold blocks (Ross and Locascio 2002). The heated copper block, whose temperature was regulated by a PID controller, was heated using a small high-power resistor embedded into the copper. To regulate the temperature of the cold zones, cold water from a thermostated bath was passed through the holes drilled within the cooled copper blocks. Similar works are also been reported by Mao and coworkers (Kinahan et al. 2009; Mao et al. 2002a, b). Although such systems can easily obtain the desired temperature gradient range, they often require an external bulky water bath and its accessorial equipment (such as temperature controller and circulating pump). As a result, they are difficult to miniaturize onto a single microfuidic device. In order to improve this, some researchers have used the metallic strips and/or thin-film heaters to generate the desired linear temperate gradient (Cheng et al. 2005; Crews et al. 2007, 2008a, b, c, 2009). A network of cooling fins was coupled to the strip corresponding to the cooler zone, and as a result a nearly linear temperature gradient could be obtained (Crews et al. 2008b). However, these experiences maybe showed a general lack of robustness in regulating the temperature gradient. In addition, these systems are complicated in the temperature control system and difficult in establishing stable and uniform temperature gradients with multiple heating sources. Recently, Zhang et al. have developed a novel temperature gradient technology using a slantwise radiative heating system (Zhang et al. 2007c). Although such approach can generate a highly reproducible temperature gradient with high spatial resolution, it lacks the flexibility to changing the temperature gradient.

In our work, the combined fin design is used to produce the desired temperature gradient. The hotter edge on the grooved copper flake (i.e. copper fin) was heated by a high-power cartridge heater, and the aluminum fin array together with the low-power fan was used to cool the heater copper fin. As a result, a temperature gradient can be obtained. Compared with the works reported previously, our temperature gradient method posses several characteristics and/or advantages as follows: (1) it does not need a circulating water bath to obtain the temperature gradient, and therefore the developed device is more compact and promises to incorporate to a single chip for biological and chemical applications; (2) the temperature gradient is easily adjusted. Only turning the knob of the DC supply powering to the fan, different temperature gradients along the copper fin can be obtained. (3) the temperature gradient is a non-linear and exponentially-decreasing one. This feature in the gradient is favorable for PCR, since the critical ramping time is between the annealing and extension temperature (Crews et al. 2008b). In addition, compared with a linear temperature gradient, the smaller reaction system can be used under similar conditions. (4) the temperature gradient obtained is little affected by varying non-temperature environmental conditions (such as gentle wind), and therefore it is highly reproducible and highly accurate. (5) insulating the surface in the temperature gradient region is unnecessary since the passive nature convection from the cover side has an active effect on the formation of the temperature gradient in our device. Figure 5 shows a series of plots of temperature versus position along the temperature gradient direction under various fan power conditions. Here, the positions at the x=0, 4.4, 8.8, 13.2, 17.6, 22.0, 26.4, 30.8, 35.2 mm are channel 1, 3, 5, 7, 9, 11, 13, 15, and 17, respectively, on the grooved copper flake. When no finned aluminum heat sink applied to the copper flake under the passive nature convection, the temperatures within the first and the 17th channel are 97± 0.1°C and 89.8±0.1°C, respectively. Apparently, this temperature range does not suit for the PCR temperature conditions. By using the finned heat sink and the natural

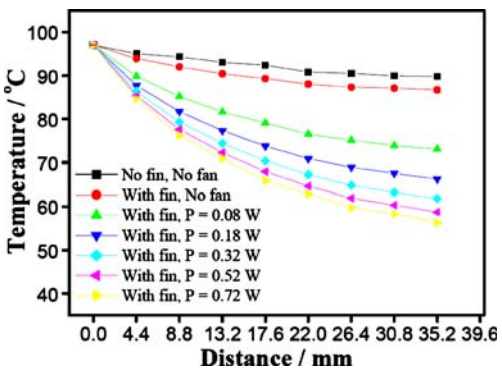

Fig. 5 A plot of temperature vs position of temperature gradient device with different fan powers at an ambient temperature of 22°C. Data are the means of three replicates and error bars for each point are shown when larger than the symbols

convection, the temperature within the 17th channel was reduced to 86.7±0.2°C, and the about 12°C temperature difference was obtained. When the used fan power ranged from 0.08 to 0.72 W, the temperature difference along the temperature gradient was gradually increased. For example, when a fan power of 0.08 W was utilized, the temperature within the 17th channel was 73.1±0.1°C. This temperature was further reduced to 56.3±0.2°C as the active cooling power was increased to 0.72 W. At this case, the temperature gradient on the copper flake spanned the range from 97 to 52°C. As a result, the temperature range on the temperature gradient device can be desirably used for the PCR amplification.

The average temperature gradient obtained in our device is approximately 1.1°C/mm. This value is higher than that reported by Ohashi and coworkers (0.58°C/mm) (Ohashi et al. 2007). However, the obtained average temperature gradient in the current device is much lower than one reported by Crews et al. (Crews et al. 2008b), that was high up to 3.5°C/mm. We attribute such results to the two following reasons: (1) the thickness of the copper flake and the base of the aluminum fin array is larger. Seen from the aforementioned governing equation, under similar conditions, the temperature difference along the temperature gradient direction on a thin fin flake is apparently larger than that obtained on a thick fin flake. (2) the thermal conductivity of temperature gradient copper plate is higher. Using a material with low thermal conductivity as a heat-conducting plate, such as ceramic, glass, or Teflon, the average temperature gradient should increase. Therefore, it is likely that the temperature difference between the hot and the cold part in our device can be significantly increased or a steep temperature gradient on a compact device can be formed.

5.2 Single-loop PCR in MG-PCR device

This study takes the single-loop PCR process as an example in order to demonstrate the successful PCR achieved using the reported temperature gradient technology. The relatively large temperature difference between the two vertical edges that are imbedded within the hot and the cold parts of the temperature gradient device, can induce significant differences in the flow density, which can be used for the fluid transport under appropriate conditions. This approach for performing flow-based PCR is called convective PCR (Braun et al. 2003; Krishnan et al. 2002). In this work, the evaluation of flow velocity within the convective loop reactor, which corresponds to the cycling times, is not the major focus. Therefore, a conservative 120 min of reaction in the MG-PCR device was first used. Figure 6 shows the comparison of single-loop MG-PCR with conventional PCR. After a reaction of 120 min on the MG-PCR device, levels of amplification obtained (lanes 6 and 7 in Fig. 6) were comparable to those (lanes 2 and 3 in Fig. 6) in a conventional gradient PCR machine using a three-temperature (35 cycles, 100-min reaction time) or two-temperature (35 cycles, 50-min reaction time) cycling protocol. It should be noted that a good way to evaluate the efficiency of a developed PCR device is to compare the real-time amplification of serially diluted sample of know concentration. However, the current MG-PCR device is not compatible with real-time detection. Therefore, estimates of efficiency and specificity were made by comparing of gel eletrophoregrams of PCR product amplified on the MG-PCR device and the control system. In Fig. 6, the single-loop PCR product in the MG-PCR device is nearly as concentrated as that of the conventional gradient PCR, comparable amplification efficiency can be assumed.

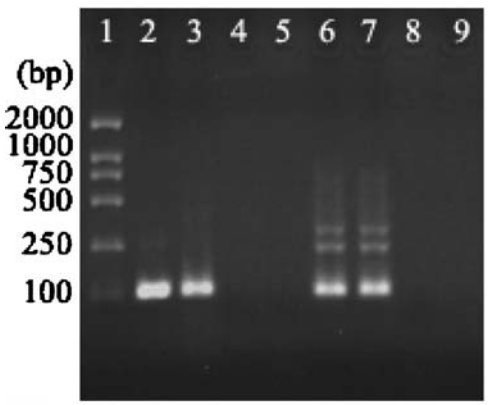

Lane	Sample
1	DNA marker
2	Conventional PCR positive (three-temperature cycling)
3	Conventional PCR positive (two-temperature cycling)
4	Conventional PCR negative without template (two-temperature cycling)
5	Conventional PCR negative without enzyme (two-temperature cycling)
6	MG-PCR positive
7	MG-PCR positive
8	MG-PCR negative without template
9	MG-PCR negative without enzyme

Fig. 6 Comparison of MG-PCR with conventional PCR. The hot and cold parts of the convective-flow loop on the MG-PCR device were maintained at 91.6±0.2°C (channel 2) and 60.5±0.2°C (channel 18). The fan was run by a 0.32 W power and all MG-PCR reactions run for 120 min. Lanes 6–7 denote MG-PCR products from two independent runs under the same reaction conditions. In the conventional two-temperature cycling protocol, the annealing temperature and extension temperature are combined together (60°C)

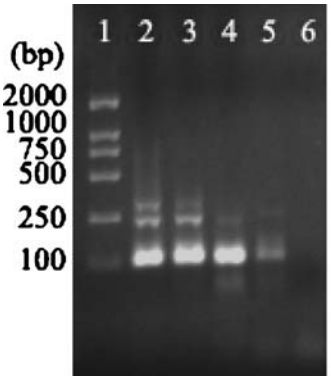

Lane	Sample
1	DNA marker
2	MG-PCR, 120 min
3	MG-PCR, 90 min
4	MG-PCR, 60 min
5	MG-PCR, 45 min
6	MG-PCR, 30 min

Fig. 7 MG-PCR amplification as a function of reaction time. During runs, the DNA template and Taq DNA polymerase concentrations were 4 ng/μl and 0.1 unit/μl

However, some non-specific products were found when 120-min and even 90-min reaction time were utilized in our device (lanes 6 and 7 in Fig. 6 and lanes 2 and 3 in Fig. 7). This is most likely due to the long reaction time resulting in the increased number of cycles. In the MG-PCR device, the reaction time could be further reduced without loss of reaction efficiency (Fig. 7). Importantly, amplification could be successfully obtained in as short as 45 min, as shown by a clear band of lane 5 in Fig. 7. However, further reducing the reaction time to 30 min did not yield amplification. We attribute this to the lack of cycle number in the loop reactor. Of course, lower yields with lower cycle numbers are a common finding in the continuous-flow PCR systems (Obeid et al. 2003) and even conventional PCR system. The current device was not optimized and a convective loop as long as 180 mm was used. As the device is improved and a shorter fluid loop is used, the cycle number in the reaction loop can be increased under similar conditions. Therefore, it is likely that the reaction time can be reduced. It is necessary to note that during the MG-PCR experiments, the same reagents were used as those in the conventional gradient PCR device, and the reaction protocol was not optimized, indicating the robustness of the MG-PCR system. The MG-PCR experiments were repeated several times with excellent reproducibility. In our device, although no attempt was made to amplify DNA target templates above 200 bp in length, it should be note that the great number of genetic testing and pathogen detection involve target sequence less than 200 bp in size. For this reason, the initial testing of the MG-PCR device focused on the lower range of target sizes. However, it is probable that the current device can amplify 3000-bp target sample since an average flow velocity of approximate 0.8 mm/s could be estimated under PCR conditions stated in Figs. 6 and 7, and therefore the residence time within each temperature zone was approximate 50 s. Here, it is generally assumed that the extension rate of Taq enzyme is 60–100 mers/s.

5.3 Multi-loop parallel PCR amplification in MG-PCR device

As stated earlier, within applications of microfluidic DNA amplification, multichamber or multichannel parallel DNA amplification has attracted great focus. However, little attention has been paid to the development of parallel DNA amplification with different annealing temperatures. In this work, the MG-PCR has been developed by using our decreasing-exponentially temperature gradient technology, and can be utilized for parallel PCR amplification with different annealing temperatures. One advantage of using the MG-PCR technology is that it is easy enough to optimize the annealing temperature parameter within microfluidic DNA

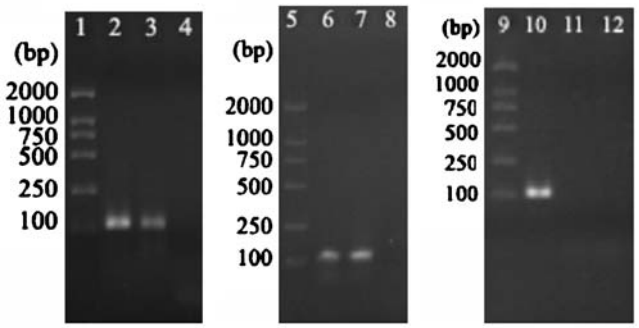

Lane	Sample
1, 5, 9	DNA marker
2	96.6 ± 0.2 °C (channel 1) / 60.5 ± 0.2 °C (channel 18), P=0.32 W
3	91.6 ± 0.2 °C (channel 2) / 63.2 ± 0.2 °C (channel 15), P=0.32 W
4	86.3 ± 0.2 °C (channel 3) / 67.2 ± 0.1 °C (channel 11), P=0.32 W
6	96.7 ± 0.2 °C (channel 1) / 67.2 ± 0.2 °C (channel 11), P=0.32 W
7	91.6 ± 0.2 °C (channel 2) / 60.6 ± 0.2 °C (channel 18), P=0.32 W
8	86.4 ± 0.2 °C (channel 3) / 63.2 ± 0.2 °C (channel 15), P=0.32 W
10	96.7 ± 0.2 °C (channel 1) / 66.2 ± 0.1 °C (channel 17), P=0.18 W
11	91.8 ± 0.2 °C (channel 2) / 71.8 ± 0.2 °C (channel 10), P=0.18 W
12	87.7 ± 0.2 °C (channel 3) / 64.8 ± 0.1 °C (channel 18), P=0.18 W

Fig. 8 Fluorescence image of MG-PCR products from three parallel reactions within three independent runs. All reactions ran in the MG-PCR device for 75 min, and the Taq polymerase concentration and initial template concentration were 0.1 unit/ μl and 4 ng/μl, respectively

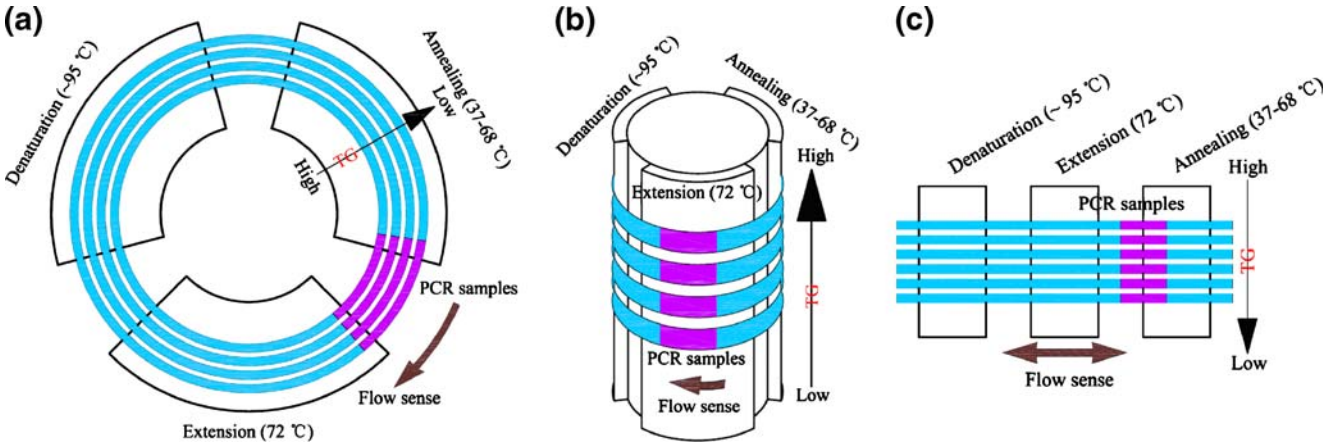

Fig. 9 Applications of the current temperature gradient technology for other potential continuous-flow MG-PCR devices for high-throughput DNA amplification. **(a)** Concentric circular channels on a planar flake; **(b)** Non-concentric circular channels on a compact cylindrical device; **(c)** Straight channels on an oscillatory-flow MG-PCR device. TG = temperature gradient

amplification. In general, due to the microscale effect of DNA amplification system, it is not reasonable that the annealing temperature optimized using the conventional PCR (or gradient PCR) device is used for that within microfluidic DNA amplification. Here, in order to demonstrate that our MG-PCR device can be utilized for parallel PCR amplification with various annealing temperatures, three near-identical reaction loops were arranged on the MG-PCR device, as is similar to that shown in Fig. 3. During experiments, the hot and cold edges of the reaction loops were imbedded within certain channels on the temperature gradient device. The flexibility of PTFE tube was utilized to construct the near-planar convective loops, and allowed the same reaction loops to be used within runs. That is to say, the three loops of same lengths are used, but they aren't completely arranged concentrically on the same plane. To do so, the upper and lower parts of the two inner loops needed to somewhat depart from the plane of the outermost loop. However, such arrangement always results in some difference in cycling time between the innermost and outermost loops. Figure 8 demonstrates the three independent experimental results of parallel PCR amplifications with different annealing temperatures in our MG-PCR device. As seen from Fig. 8, the MG-PCR performed well within the annealing temperature ranging from 60 to 68°C (lanes 6 and 7 in Fig. 8). The results obtained in the MG-PCR device were consistent with those obtained from a commercial gradient PCR thermocycler (data not shown). However, further increasing the annealing temperature to ~72°C did not yield PCR amplification (lane 11 in Fig. 8), probably due to imperfect primer annealing. In addition, the PCR within the innermost loop did not success during each parallel run (lanes 4, 8, and 12 in Fig. 8). This probably is attributed to low denaturation temperature, which is less than 90°C. In our MG-PCR device, performing parallel PCR with different annealing temperatures not only saves labor and working time, but also

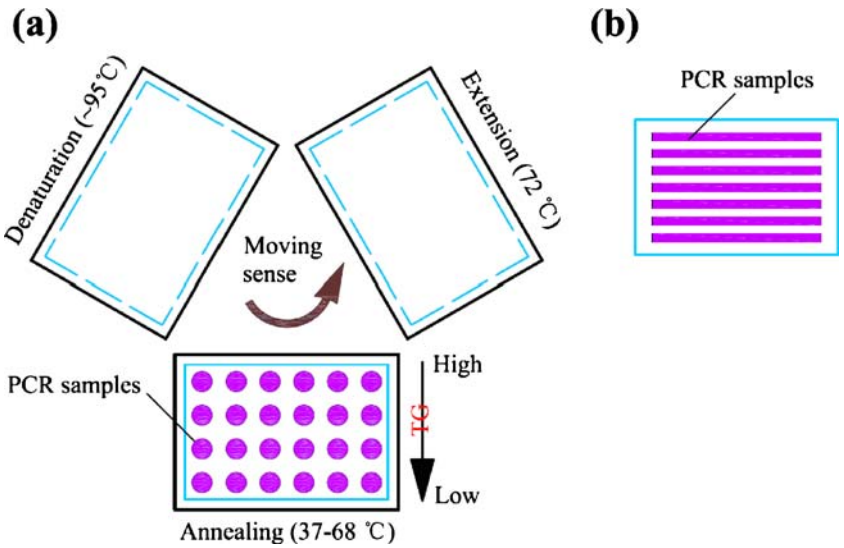

Fig. 10 Applications of the current temperature gradient technology for other potential stationary-chamber MG-PCR devices for high-throughput DNA amplification. **(a)** A chamber reaction array on a chip is moved between three temperature zones for MG-PCR amplification; **(b)** The channel reaction array on a chip substituting for on-chip chamber reaction array. TG = temperature gradient

increases the versatility and flexibility. However, our prototype device can not perform high-throughput (for example four or even higher) parallel PCR reactions with different annealing temperatures. This is because of the narrow denaturation zone on the temperature gradient device. In order to circumvent this shortcoming, some approaches can be utilized as follows: (1) the width between two adjacent grooves at the hot region is reduced to increase the number of channels; (2) a grooved copper flake with changeable cross-sectional area can be constructed. At the hot zone the cross-sectional area is somewhat larger than that at the cold zone, and therefore the temperature gradient at the hot zone can be reduced; (3) the finned heat sink is far away from the hot region and the temperature gradient at the hot region will be reduced. By using these approaches, some improved designs are now being tested to reduce the temperature gradient in the hot region, and further increase the reaction throughput of the MG-PCR device. The improved design can provide a powerful MG-PCR amplification.

6 Extensions of method

In our preliminary MG-PCR device, the reaction throughput is low, and such throughput can not meet the requirements of nucleic acid amplification and analysis. However, the temperature gradient technology and the MG-PCR method reported herein can be extended to other microfluidic DNA amplification systems. When the temperature gradient flake developed in this work is used as the specific annealing zone within the continuous-flow PCR systems, the MG-PCR amplification throughput can be significantly increased. As an example, Fig. 9 demonstrates potential applications of the current temperature gradient technology for other continuous-flow MG-PCR devices for high-throughput PCR amplification. In Fig. 9(a), the concentric circular PCR reaction channels on a planar flake are placed on the three temperature zone. Figure 9(b) shows that the non-concentric same circular PCR channels can be arranged onto a compact cylindrical device, and Fig. 9(c) illustrates the straight MG-PCR reaction channels on an oscillatory-flow device. Within these potential MG-PCR devices, the annealing temperature may range from 37 to 68°C and even the wider range of annealing temperature can be used. In addition, the MG-PCR amplification throughput is completely dependent on the number of reaction channel, and therefore such throughput can be desirably increased by the user. Of course, the current temperature gradient technology can also be applied onto other stationary-chamber MG-PCR devices for high-throughput DNA amplification (Fig. 10). It should be noted that the current temperature gradient device can be down-scaled, and therefore can be applied onto the chip-based PCR amplification systems.

Within the MG-PCR device reported herein, the natural convection pumping mechanism is used to drive the fluid flow in the reaction loop. Although this pump is simple and inexpensive in design, it has some limits in application. For example, the flow rate within the reaction loop is largely dependent upon the inner diameter of the loop and the temperature difference between the PCR temperature zones. Fortunately, a number of mechanical (piezoelectric, pneumatic, and thermopneumatic) and non-mechanical (electrokinetic, magnetohydrodynamic, electrochemical, acoustic-wave, surface tension and capillary, and ferro-fluidic magnetic) micropumps have been successfully used within PCR chips (Zhang et al. 2007a). In the future, these micropumps are likely applied to the current MG-PCR device. In addition, as stated earlier, the temperature gradient devices have been successfully applied for many microfluidic DNA analysis applications. Therefore, it is likely that our current temperature gradient device is used for these applications.

7 Conclusions

We constructed a MG-PCR system with a non-linear temperature gradient formed on a combined finned copper flake. We have shown that the newly developed system is capable of performing parallel PCR amplifications with different annealing temperatures ranging from 60 to 68°C. Compared with the conventional gradient PCR machine, the current MG-PCR device has several obvious advantages, including simple and inexpensive device design, faster amplification rates, flexible incorporation with existing laboratory protocols and fluid handling systems, and easy operation in a portable, low-consumption fashion. Within future MG-PCR device, real-time fluorescence detection or other detection technology such as CE is likely integrated to provide on-line MG-PCR product detection. We expect to be only at the beginning of the MG-PCR development that will have great impact on the field of microfluidic DNA amplification in further years.

Acknowledgements This research is supported by the National Natural Science Foundation of China (30700155; 30870676; 30800261), the Program for Changjiang Scholars and Innovative Research Team in University (IRT0829) and the National High Technology Research and Development Program of China (863 Program) (2007AA10Z204).

References

P. Baaske, S. Duhr, D. Braun, Appl. Phys. Lett. **91**, 133901 (2007)
K.M. Balss, D. Ross, H.C. Begley, K.G. Olsen, M.J. Tarlov, J. Am. Chem. Soc **126**, 13474–13479 (2004)

D. Braun, N.L. Goddard, A. Libchaber, Phys. Rev. Lett. **91**, 158103 (2003)
J.S. Buch, C. Kimball, F. Rosenberger, W.E. Highsmith Jr. D.L. DeVoe, C.S. Lee, Anal. Chem. **76**, 874–881 (2004)
J.S. Buch, F. Rosenberger, W.E. Highsmith Jr. C. Kimball, D.L. DeVoe, C.S. Lee, Lab Chip **5**, 392–400 (2005)
M. Chabert, K.D. Dorfman, P. de Cremoux, J. Roeraade, J.L. Viovy, Anal. Chem. **78**, 7722–7728 (2006)
M. Chang, H.J. Lee, Anal. Biochem. **340**, 174–177 (2005)
J.Y. Cheng, C.J. Hsieh, Y.C. Chuang, J.R. Hsieh, Analyst **130**, 931–940 (2005)
N. Crews, T. Ameel, C. Wittwer, B. Gale, Lab Chip **8**, 1922–1929 (2008a)
N. Crews, C. Wittwer, B. Gale, Proc. SPIE **6465**, 646504 (2007)
N. Crews, C. Wittwer, B. Gale, Biomed. Microdevices **10**, 187–195 (2008b)
N. Crews, C. Wittwer, R. Palais, B. Gale, Lab Chip **8**, 919–924 (2008c)
N. Crews, C.T. Wittwer, J. Montgomery, R. Pryor, B. Gale, Anal. Chem. **81**, 2053–2058 (2009)
M. Curcio, J. Roeraade, Anal. Chem. **75**, 1–7 (2003)
K.D. Dorfman, M. Chabert, J.H. Codarbox, G. Rousseau, P. de Cremoux, J.L. Viovy, Anal. Chem. **77**, 3700–3704 (2005)
S. Duhr, D. Braun, Proc. Natl. Acad. Sci. U. S. A. **103**, 19678–19682 (2006)
H.C. Fan, S.R. Quake, Anal. Chem. **79**, 7576–7579 (2007)
J. Grover, R.D. Juncosa, N. Stoffel, M. Boysel, A.I. Brooks, M.P. McLoughlin, D.W. Robbins, IEEE Sens. J. **8**, 476–487 (2008)
T. Kajiyama, Y. Miyahara, L.J. Kricka, P. Wilding, D.J. Graves, S. Surrey, P. Fortina, Genome Res. **13**, 467–475 (2003)
D.J. Kinahan, T.M. Dalton, M.R.D. Davies, Biomed. Microdevices **11**(4), 747–754 (2009)
M.M. Kiss, L. Ortoleva-Donnelly, N.R. Beer, J. Warner, C.G. Bailey, B.W. Colston, J.M. Rothberg, D.R. Link, J.H. Leamon, Anal. Chem. **80**, 8975–8981 (2008)
M.U. Kopp, A.J. de Mello, A. Manz, Science **280**, 1046–1048 (1998)
M. Krishnan, V.M. Ugaz, M.A. Burns, Science **298**, 793 (2002)
Y.Y. Li, D. Xing, C.S. Zhang, Anal. Biochem. **385**, 42–49 (2009)
H. Mao, M.A. Holden, M. You, P.S. Cremer, Anal. Chem **74**, 5071–5075 (2002a)
H. Mao, T. Yang, P.S. Cremer, J. Am, Chem. Soc. **124**, 4432–4435 (2002b)
T. Morrison, J. Hurley, J. Garcia, K. Yoder, A. Katz, D. Roberts, J. Cho, T. Kanigan, S.E. Ilyin, D. Horowitz, J.M. Dixon, C.J. Brenan, Nucleic Acids Res. **34**, e123 (2006)
H. Nagai, Y. Murakami, K. Yokoyama, E. Tamiya, Biosens. Bioelectron **16**, 1015–1019 (2001)
P.J. Obeid, T.K. Christopoulos, H.J. Crabtree, C.J. Backhouse, Anal. Chem. **75**, 288–295 (2003)
T. Ohashi, H. Kuyama, N. Hanafusa, Y. Togawa, Biomed. Microdevices **9**, 695–702 (2007)
V.C. Padmakumar, R. Varadarajan, Anal. Biochem. **314**, 310–315 (2003)
N. Park, S. Kim, H. Hahn, Anal. Chem. **75**, 6029–6033 (2003)
D. Ross, L.E. Locascio, Anal. Chem. **74**, 2556–2564 (2002)
W. Rychlik, W.J. Spencer, R.E. Rhoads, Nucleic Acids Res. **18**, 6409–6412 (1990)
Y. Schaerli, R.C. Wootton, T. Robinson, V. Stein, C. Dunsby, M.A. Neil, P.M. French, A.J. Demello, C. Abell, F. Hollfelder, Anal. Chem. **81**, 302–306 (2009)
Y.H. Shim, C.D. Park, D.H. Kim, J.H. Cho, M.H. Cho, H.J. Kim, Biol. Pharm. Bull. **28**, 671–676 (2005)
N. Stoffel, A. Fisher, S.S. Tan, M. Boysel, Proceedings of 57th Electronic Components & Technology Conference, Reno, NV, 2007, pp, 1561-1566 (2007)
Y. Sun, N.T. Nguyen, Y.C. Kwok, Anal. Chem. **80**, 6127–6130 (2008)
W. Sybesma, J. Hugenholtz, I. Mierau, M. Kleerebezem, Biotechniques **31**, 466, 468, 470, 472 (2001)
P. Wilding, M.A. Shoffner, L.J. Kricka, Clin. Chem. **40**, 1815–1818 (1994)
D.Y. Wu, L. Ugozzoli, B.K. Pal, J. Qian, R.B. Wallace, DNA Cell Biol. **10**, 233–238 (1991)
C.S. Zhang, D. Xing, Nucleic Acids Res. **35**, 4223–4237 (2007)
C.S. Zhang, D. Xing, Y.Y. Li, Biotechnol. Adv. **25**, 483–514 (2007a)
C.S. Zhang, J.L. Xu, W.L. Ma, W.L. Zheng, Biotechnol. Adv. **24**, 243–284 (2006)
C.S. Zhang, J.L. Xu, J.Q. Wang, H.P. Wang, Anal. Lett. **40**, 497–511 (2007b)
H.D. Zhang, J. Zhou, Z.R. Xu, J. Song, J. Dai, J. Fang, Z.L. Fang, Lab Chip **7**, 1162–1167 (2007c)